Development 134, 2615-2625 (2007) doi:10.1242/dev.000877

Defective osteoblast function in ICAP-1-deficient mice

Daniel Bouvard[1,2,3,*], Attila Aszodi[3], Günter Kostka[3], Marc R. Block[1,2], Corinne Albigès-Rizo[1,2] and Reinhard Fässler[3]

The integrin receptor family plays important roles in cell-to-cell and cell-to-extracellular matrix interactions through the recruitment of accessory molecules. One of them, the integrin cytoplasmic domain-associated protein-1 (ICAP-1; also known as ITGB1BP1), specifically interacts with the cytoplasmic domain of the β_1 integrin subunit and negatively regulates its function in vitro. To address the role of ICAP-1 in vivo, we ablated the *Icap-1* gene in mice. We report an unexpected role of ICAP-1 in osteoblast function during bone development. *Icap-1*-deficient mice suffer from reduced osteoblast proliferation and delayed bone mineralization, resulting in the retarded formation of bone sutures. In vitro studies reveal that primary and immortalized *Icap-1*-null osteoblasts display enhanced adhesion and spreading on extracellular matrix substrates, probably owing to an increase in β_1 integrin activation. Finally, we provide evidence that ICAP-1 promotes differentiation of osteoprogenitors by supporting their condensation through modulating the integrin high affinity state.

KEY WORDS: ICAP-1 (ITGB1BP1), Integrin, Cell differentiation, Cell adhesion, Osteoblast, Mouse

INTRODUCTION

Cell anchorages to extracellular matrix (ECM) and surrounding cells control shape, migration, survival and proliferation. Integrins are a large family of adhesion receptors that mediate cell-matrix and cell-cell interactions (Brakebusch et al., 2002; Hynes, 1992; Hynes, 2002). Integrins are bi-directional signaling molecules, which switch between a low (inactive) and a high affinity (active) state. The switch to the high affinity state is controlled by intracellular signals that act on the cytoplasmic domain of integrins and induce rapid and reversible changes in the conformation of the integrin extracellular domains (inside-out signal) (Calderwood, 2004). Following activation, integrins bind their ligands, merge into large clusters, recruit a multitude of proteins to form so called focal adhesions (FAs), and transmit signals to various subcellular compartments (outside-in signal).

ICAP-1 [integrin cytoplasmic domain associated protein-1; also known as integrin beta 1 binding protein 1 (ITGB1BP1)] is a ubiquitously expressed protein identified in a yeast two-hybrid screen as a β_1 integrin cytoplasmic domain-interacting protein (Chang et al., 1997). Human cells express two *ICAP-1* isoforms that are generated by alternative splicing. The large isoform associates with the cytoplasmic tail of β_1 integrin. The small isoform lacks a C-terminally located integrin-binding site (Chang et al., 1997) and is therefore unable to interact with β_1 integrin. Overexpression of ICAP-1 negatively regulates β_1 integrin function by diminishing the strength of adhesion to, and enhancing cell migration on, fibronectin (FN) (Bouvard and Block, 1998; Bouvard et al., 2003; Zhang and Hemler, 1999). How ICAP-1 exerts its functional properties is still unclear. One study proposed direct competition with talin for binding to β_1 integrin (Bouvard et al., 2003). Talin is a large cytoplasmic protein that binds and activates several integrins, and links them to the actin cytoskeleton (Calderwood et al., 2002; Vinogradova et al., 2002). Recruitment of ICAP-1 on β_1 integrin would dislodge talin and thereby reduce the affinity state of β_1 integrins leading to FA disassembly (Bouvard et al., 2003). In line with this hypothesis is the finding that ICAP-1 is absent from FAs. A second study suggests that ICAP-1 might act as a guanine dissociation inhibitor (GDI) for the small GTPases RAC1 and CDC42 (Degani et al., 2002). A reduced RAC1 and/or CDC42 activity could also explain the spreading defects of cells overexpressing ICAP-1 (Bouvard et al., 2003; Degani et al., 2002).

Finally, the identification of additional binding partners such as KRIT1 and the nucleotide diphosphate kinase NM23-H2 (also known as NME2) (Fournier et al., 2002; Zawistowski et al., 2002; Zhang et al., 2001) linked ICAP-1 to additional signaling pathways. Loss-of-function mutations in *KRIT1* cause a human disease called cerebral cavernous malformation type I (Laberge-le Couteulx et al., 1999), which is characterized by abnormalities of the brain vasculature. KRIT1 has been shown to bind microtubules and the small GTPase RAP1A (Gunel et al., 2002; Serebriiskii et al., 1997). RAP1A can reverse the transformed phenotype of KRAS-overexpressing cells and modulate integrin-mediated cell adhesion on FN (Bos et al., 2001). NM23-H2 is a protein with nucleoside diphosphate kinase activity that has been linked to a variety of cellular activities including the suppression of metastasis and cell motility of tumour cells in vitro. NM23-H2 can bind to the promoter sequences of the *PDGFA* and *c-Myc* (*MYC* – Human Gene Nomenclature Database) genes, modulate the activity of small GTPases such as RAD (also known as RRAD) and RAC1, and localizes in cell ruffles upon integrin ligation (Fournier et al., 2002).

To directly test the function of ICAP-1 in vivo, we generated *Icap-1*-deficient mice. Most of the mutant mice are born and develop craniofacial dysmorphism and dwarfism caused by abnormal proliferation and differentiation of osteoblasts leading to a delayed closure of calvarial sutures. Furthermore, we show that ICAP-1 regulates β_1 integrin activity and the condensation of preosteoblastic cells, an absolute requirement for proper bone development.

MATERIALS AND METHODS

Generation of *Icap-1*-deficient mice

Five positive PAC clones were isolated from an RPCI21 library and used to generate the targeting construct (details available on request). Electroporation into passage-13 R1 ES cells was performed as previously described (Talts et al., 1999). Mice were genotyped by Southern blot or by PCR.

[1]Université Joseph Fourier, CNRS, UMR 5538, LEDAC, Institut Albert Bonniot, La Tronche Cedex, F-38706, France. [2]INSERM, U823, Equipe DySAD, Institut Albert Bonniot, F-38042, France. [3]Max Planck Institut für Biochemie, Department of Molecular Medicine, Am Klopferspitz 18a, 82152 Martinsried, Germany.

*Author for correspondence (e-mail: daniel.bouvard@ujf-grenoble.fr)

Accepted 4 May 2007

Antibodies

Polyclonal anti-ICAP-1 antibodies were described previously (Bouvard and Block, 1998). Monoclonal antibodies against actin, vinculin (clone hVIN1) and talin (clone 8d4) were from Sigma-Aldrich (Germany). Polyclonal anti-β_1 integrin serum was a gift from Dr Johansson (The Biomedical Center, Uppsala University, Sweden). Monoclonal β_1 antibodies 9EG7 and MB1.2 were from Pharmingen (France) and a gift from Dr Bosco (Robarts Research Institute, Ontario, Canada), respectively. Polyclonal anti-collagen I, III and osteonectin/BM-40 antibodies were from Dr R. Timpl (Max Planck Institute for Biochemistry, Martinsried, Germany). Polyclonal antibodies against cyclin D1, FGFR1 and FGFR3 were from SantaCruz (USA), against Ki67 from Novocastra (UK) and against 5-bromo-2′-deoxyuridine (BrdU) from Roche (Germany).

Isolation and assays with primary osteoblasts

A primary mouse osteoblast-enriched cell population was isolated from newborn calvaria using a mixture of 0.3 mg/ml collagenase type I (Sigma) and 0.25% trypsin (Gibco BRL) as described previously (Bellows et al., 1986; Otto et al., 1996). Cells were grown in α-MEM medium containing 10% FCS.

In vitro differentiation of isolated osteoblasts was performed essentially as described (Globus et al., 1998). Briefly, 60,000 cells per well were plated in a 24-well tray. After 3 days of culture, when cells were confluent, the medium was switched to differentiation medium (α-MEM, 10% FBS, 50 μg/ml ascorbic acid, 10 mM β-glycerophosphate) and changed every second day. The differentiation process was visualized by alkaline phosphatase (AP) staining for osteoblast activity and by Alizarin Red S staining for calcium deposition.

For the adhesion assay, primary osteoblasts (passage 2) were seeded at 0.5×10^5 cells in a 96-well tray coated with various concentrations of FN or COL1. The cells were incubated for 1 hour at 37°C and then washed three times with PBS before staining with a Crystal Violet solution (0.1% Crystal Violet, 20% methanol) for 1 hour at room temperature. After three washes in water, cells were lysed in 0.1% SDS for 1 hour. The absorbance was read at 550 nm with a Beckman Coulter AD 340 absorbance detector.

Cell proliferation was estimated by the BrdU assay as previously described (Fournier et al., 2005).

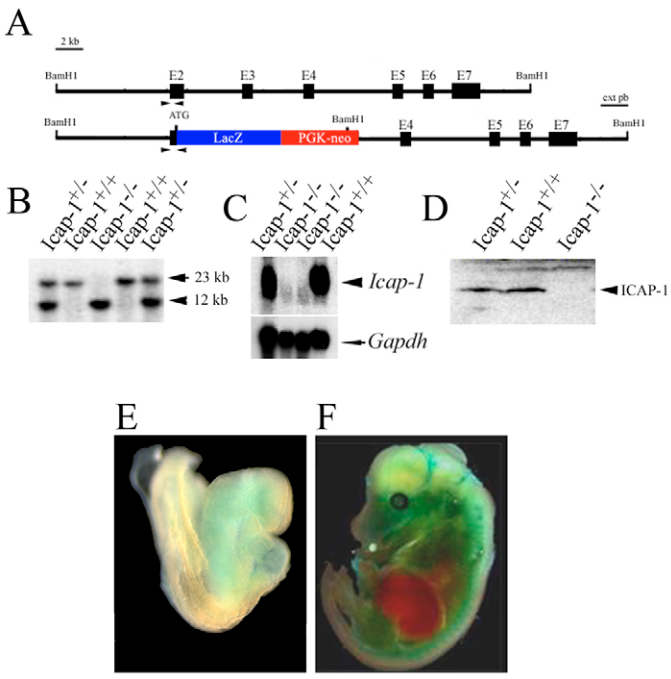

Fig. 1. Disruption of the mouse *Icap-1* gene. (**A**) Partial structure of the mouse *Icap-1* gene and the targeted allele after homologous recombination. Black boxes represent exons (E2 to E7). The initiation codon (ATG) is located in exon 2. The expected fragment sizes for wild-type and recombinant alleles are 20 and 10 kb, respectively, following digestion with *Bam*HI and hybridization with the indicated external probe (ext pb). (**B**) Southern blot analysis of tail DNA isolated from wild-type, heterozygous mutant and homozygous mutant mice. (**C**) Northern blot analysis of total RNA derived from adult kidney of wild-type, heterozygous and homozygous mutant mice. The filter was hybridized with probes specific for *Icap-1* and *Gapdh*, respectively. (**D**) Western blot analysis of wild-type, heterozygous and homozygous mutant brain extracts. (**E**,**F**) Whole-mount *lacZ* staining of heterozygous mutant embryos at E8.5 (E) and E14.5 (F).

Immortalization of osteoblasts

Primary osteoblasts (passage 2) were infected with a retrovirus expressing the large SV40 T antigen (Fässler et al., 1995), cloned and tested for their ability to induce AP upon differentiation (Mansukhani et al., 2000). Clone SV2.1 from an *Icap-1*-deficient mouse and clone SV6.5 from a wild-type animal were used. Rescue of ICAP-1 expression in SV2.1 cells was via retroviral infection using the pCLMFG-*Icap*-IRES-EGFP vector. A homogeneous cell population was sorted based on EGFP fluorescence with a MoFlo cell sorter (Dako Cytomation). ICAP-1 expression was checked by western blot, immunofluorescence and FACS using EGFP as a marker. This non-clonal cell population is referred to as SV2.1-*Icap-1*^{resc} hereafter.

Compaction assay in hanging drops

Immortalized cells were harvested by trypsin digestion and washed twice in DMEM medium. Drops of 10 μl of DMEM-SVF medium containing 25,000 cells were spotted onto the cover lid of 10 cm Petri dishes, inverted and placed on a Petri dish containing 8 ml of PBS. Spheroid compaction was then followed over a 72-hour incubation period and images taken with a binocular microscope equipped with a digital camera.

Skeletal preparation, X-Gal staining and X-ray analysis

Staining of whole-mount embryos with Alcian Blue/Alizarin Red (Aszodi et al., 1998) and X-Gal (Sakai et al., 2001) was carried out as described previously. X-ray images were obtained on a dual energy setup developed at CEA/LETI (Grenoble, France).

Whole-mount in situ hybridization, histology, immunohistochemistry and in vivo cell proliferation

Whole-mount in situ hybridization was performed as described (Rice et al., 2000). Histochemistry and immunostaining on tissue sections were carried out as described (Aszodi et al., 1998). In vivo cell proliferation was analyzed using either the BrdU incorporation assay (Aszodi et al., 1998) or Ki67 immunohistochemistry. To detect cells with AP activity, calvarial cryosections were fixed for 10 minutes in 3% paraformaldehyde. After washing in PBS, the color reaction was developed in the BCIP/NBT substrate solution (Roche, France). Immunofluorescence staining and FACS analysis of primary osteoblasts were performed as previously described (Bouvard et al., 2003).

Activation index of β_1 integrin on primary osteoblasts

Activation index (AI) of β_1 integrin was estimated essentially as previously described (Calderwood et al., 2004). Briefly, primary osteoblasts were isolated and passage-2 cells were aliquoted into two pools containing either Tyrode's buffer alone or Tyrode's buffer supplemented with 5 mM EDTA. After a 15-minute incubation at 4°C, cells were incubated with or without the FITC labeled Fn7-10 fragment for 45 minutes at 4°C in the presence or absence of 5 mM EDTA, washed in ice-cold Tyrode's and analyzed on a FACScan (Becton Dickinson) flow cytometer. The collected data were analyzed using CellQuest software (Becton Dickinson). In parallel, cells were analyzed for β_1 expression using the MB1.2 monoclonal antibody to detect the level of β_1 integrin on the cell surface. The AI was calculated as follows: each specific mean intensity fluorescence (MFI) was calculated by subtracting the background obtained with Fn7-10 fragment incubation in the presence of EDTA or without the primary antibody in the case of the MB1.2 labeling. AI=[(MFI Fn7-10)-(MFI Fn7-10+EDTA)]/(MFI MB1.2)–(MFI MB1.2 control).

RNA and protein analyses

Total RNA was isolated from adult kidney using TRIzol reagent (Gibco BRL) according to the manufacturer's recommendations. For northern analysis, 10 μg of total RNA was separated on a 1.2% agarose-2.2 M formaldehyde gel, transferred to Hybond+ membrane (Amersham) and probed with a ^{32}P-labeled *Icap-1* cDNA.

For biochemistry, brains of adult mice were homogenized in RIPA buffer (10% w/v) and used for western blotting as described (Bouvard et al., 1998).

RESULTS

Generation of *Icap-1*-deficient mice

Three PAC clones containing the mouse *Icap-1* gene (also known as *Itgb1bp1* and *Bodenin*) were isolated and characterized. The *Icap-1* gene spans over 20 kb and comprises 7 exons (Fig. 1A). The transcription initiation and stop codon are located in exons 2 and 7, respectively. In human, two ICAP-1 isoforms have been identified: ICAP-1α corresponding to the full-length protein (200 amino acids) and ICAP-1β representing a shorter, 150-amino acid protein. The short isoform results from alternative splicing of exon 6, which contains the β_1 integrin-binding site (Chang et al., 1997). In mice, we were unable to detect the short isoform using RT-PCR amplification of RNA isolated form different adult tissues (data not shown). Furthermore, searches of EST and UCSC genome annotated databases also did not provide evidence of a mouse *Icap-1β*. By computer BLAST search, the gene encoding ICAP-1 was localized on mouse chromosome 12 and on human chromosome 2.

To study the in vivo function of ICAP-1, we generated an *Icap-1*-null allele by homologous recombination. The targeting strategy made use of a *lacZ* gene inserted in frame with the endogenous ATG and deleted exons 2 and 3 preventing the expression of a functional ICAP-1 protein (Fig. 1). Three correctly targeted embryonic stem (ES) cell clones were used to generate germline chimeric males. The null mutation was confirmed by Southern, northern and western blot analyses (Fig. 1B-D). Neither the *Icap-1* mRNA nor the ICAP-1 protein were detected in tissues derived from homozygous mutant (*Icap-1*$^{-/-}$) mice.

To determine the expression pattern of ICAP-1, heterozygous animals (*Icap-1*$^{+/-}$) were collected at various embryonic and adult stages and subjected to β-galactosidase (β-gal) histochemistry (Fig. 1E,F). At embryonic day 8.5 (E8.5), whole-mount staining demonstrated a faint β-gal activity in the developing heart and facial mesenchyme (Fig. 1E). At later stages, β-gal activity became gradually visible all over the embryo with the exception of the liver (Fig. 1F). On tissue sections, only a moderate β-gal activity was observed in liver, spleen, thymus and intestinal epithelial cells, whereas other tissues expressed high β-gal levels (data not shown). These results are in agreement with previously published expression data (Faisst and Gruss, 1998).

Icap-1$^{+/-}$ mice appeared normal. Southern blot genotyping of newborn mice from heterozygous intercrosses resulted in a normal number of homozygous mutants, suggesting that ICAP-1 has no rate-limiting function until birth. However, when the mendelian ratio

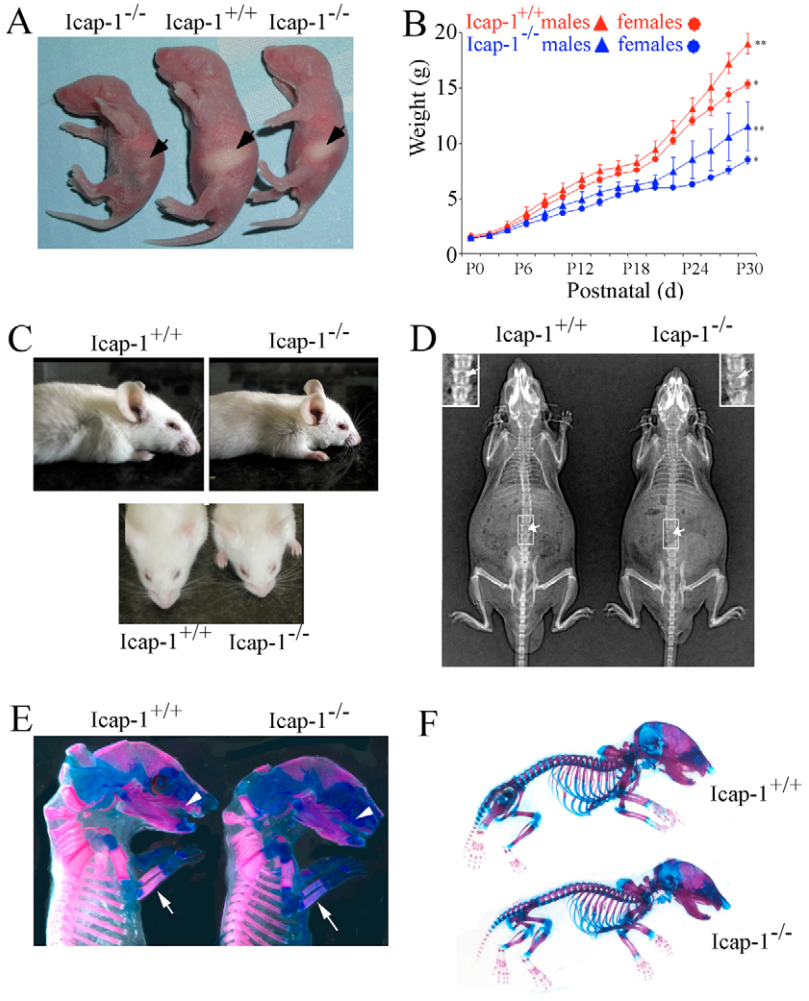

Fig. 2. Growth delay, craniofacial malformation and delayed bone mineralization in *Icap-1*-deficient mice. (**A**) Gross appearance of *Icap-1*$^{+/+}$ and *Icap-1*$^{-/-}$ P0 littermates. Note that *Icap-1*$^{-/-}$ mice are smaller in size than their control littermates. A subset of the *Icap-1*$^{-/-}$ offspring has an empty stomach (arrow). (**B**) Growth curves of control (*Icap-1*$^{+/+}$ or *Icap-1*$^{+/-}$) versus *Icap-1*$^{-/-}$ (male and female) offspring of two pooled representative littermates. Mice were weighed every other day over a period of 34 days. Each point represents the mean±s.d. (**C**) Lateral view (upper panel) or top view (lower panel) of 30-day-old wild-type and *Icap-1*-deficient mice. Note the abnormal shape (short nose and bulged-head) of the *Icap-1*-deficient skull compared with the wild type. (**D**) X-ray analysis of *Icap-1*$^{+/+}$ and *Icap-1*$^{-/-}$ 5.5-month-old mice. Note that in the *Icap-1*-null mouse the skull shape is severely affected, long bones are shorter and vertebrae are only poorly ossified (arrows and insets for higher magnification). (**E**) Alizarin Red/Alcian Blue staining of E16.5 skeletons showing reduced Alizarin Red staining intensity of the maxilla (arrowheads), the radius and ulna of the forelimb (arrows) in *Icap-1*-null tissues. (**F**) Alizarin red/Alcian Blue skeletal staining at newborn stage. No obvious difference in staining intensity or patterning could be seen between the two genotypes.

Table 1. Mendelian distribution of *Icap-1* progeny

Crossing	Wild type	Heterozygous	*Icap-1* null
***Icap-1*$^{+/-}$ × *Icap-1*$^{+/-}$**			
Expected	25	50	25
P0 (*n*=128)	27	49	24
P28 (*n*=213)	27	53	20
***Icap-1*$^{+/-}$ × *Icap-1*$^{-/-}$**			
Expected	–	50	50
P28 (*n*=34)	–	60	40

Values indicate the expected and actual (P, postnatal day) percentage of progeny of each genotype for each crossing.

of 4-week old litters from *Icap-1*$^{+/-}$ × *Icap-1*$^{+/-}$ and *Icap-1*$^{+/-}$ × *Icap-1*$^{-/-}$ intercrosses was evaluated, 20% of *Icap-1*$^{-/-}$ mice were missing (Table 1). The reason for this perinatal lethality is unknown.

Growth retardation and skeletal defects in *Icap-1*$^{-/-}$ mice

Homozygous mutant mice were slightly smaller at birth compared with wild-type littermates (Fig. 2A), and this disparity in size increased progressively postnatally. Fourteen days after birth (P14), *Icap-1*$^{-/-}$ mice were 5-10% shorter and weighed 20-50% less than control mice. These differences were maintained throughout life (Fig. 2B and data not shown). At around 3 weeks of age, *Icap-1*$^{-/-}$ mice developed obvious craniofacial abnormalities characterized by a domed skull, a shortened and broadened snout and bulged eyes (Fig. 2C). X-ray analysis of 5.5-month-old mutant mice revealed several additional abnormalities (Fig. 2D). The vault of the skull was shortened and rounded and the processus spinosus of the vertebrae was poorly ossified (Fig. 2D and inset). In the appendicular skeleton, the long bones had apparently normal bone density but were about 12-23% shorter than in control mice. These morphological defects were observed in outbred (mixed C57Bl6/Sv129J) as well as inbred (CD1 and C57Bl6) lines indicating that they occurred independently of the genetic background.

Delayed ossification in *Icap-1*$^{-/-}$ embryos

To analyze cartilaginous and bony tissues, the skeletons of homozygous mutant and wild-type animals were stained at various developmental stages with Alcian Blue (which stains cartilage) and Alizarin Red (which stains calcified tissue). The Alcian Blue staining was indistinguishable between mutant and control embryos throughout development, suggesting that cartilage formation is not grossly affected in *Icap-1*-deficient mice (Fig. 2E,F). The Alizarin Red staining, however, was reduced in the skeleton of *Icap-1*$^{-/-}$ mice as early as E14.5, indicating a defect in ossification. The reduced Alizarin Red staining was most pronounced in the parietal and frontal bones of the calvaria and in the maxillary and mandibular components of the facial skeleton (not shown). At E16.5, the reduction in Alizarin Red staining became even more prominent in the skull and in the bony collar surrounding the long bones of the appendicular skeleton (Fig. 2E).

At the newborn stage, Alizarin Red staining of long bones was similar between control and *Icap-1*$^{-/-}$ animals (Fig. 2F), suggesting that the ossification of the collar started late in *Icap-1*$^{-/-}$ mice, but was catching up at later stages. In the skull region, the postnatal development of the chondrocranium (the majority of the base of the skull) was normal in *Icap-1*$^{-/-}$ mice. This was shown by the normal ossification of the exoccipital, basioccipital, basisphenoid and presphenoid bones (Fig. 3A) and the normal formation and development of the synchondrosis of the skull base

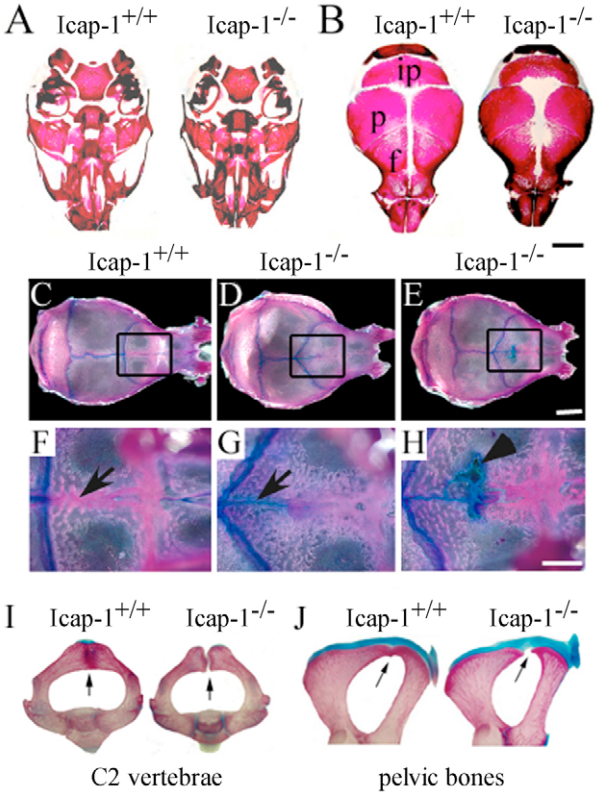

Fig. 3. Defect of calvarial ossification in *Icap-1* mutant mice. (**A**,**B**) Whole-mount Alizarin Red staining of the skulls of *Icap-1*$^{+/+}$ and *Icap-1*$^{-/-}$ newborn mice. (A) Mineralization of the skull base is comparable in wild-type and mutant animals. (B) Mineralization of the skull vault. The mineralized areas of the interparietal (ip), parietal (p) and frontal bones (f) are smaller and fontanelles are open in *Icap-1*$^{-/-}$ mice. (**C-H**) Whole-mount Alizarin Red/Alcian Blue staining of wild-type and *Icap1*-null 2-month-old calvariae. The area of the metopic suture is boxed in C-E, and displayed at high magnification in F-H. In *Icap1*-null mice (D,E), the sagittal suture is shorter, the coronal sutures are V-shaped and irregular as compared with wild-type littermates (C). At this age, the metopic suture (arrow) is closed in wild type (F), whereas in *Icap-1*-deficient mice the posterior part of the metopic suture is not ossified and is stained with Alcian Blue (G,H). Some *Icap-1*$^{-/-}$ mice display non-mineralized, Alcian Blue-positive areas in the frontal bones (arrowhead in H). (**I**,**J**) Whole-mount skeletal staining of the axis (I) and the pelvic region (J) of 21-day-old wild-type and *Icap-1*$^{-/-}$ (mt) mice. Arrows point to the fusion defect observed in the *Icap-1*-deficient mice, whereas fusion is completed in control animals. Scale bars: 2 mm in A,B; 5 mm in C-E; 2 mm in F-H.

in newborn, P15, P21 and P60 control *Icap-1*$^{-/-}$ animals (Fig. 3A and data not shown). The ossification defect of calvarial bones, however, was obvious in newborn *Icap-1*$^{-/-}$ mice (Fig. 3B). The frontal, parietal and interparietal (supraoccipital) bones were reduced in size, giving rise to enlarged anterior and posterior fontanelles and to widened sagittal and metopic (interfrontal) sutures (Fig. 3B). At the age of 2 months, control mice had completed the ossification of the metopic sutures but still had patent lambdoid, sagittal and coronal sutures (Fig. 3C,F). In mutant mice of the same age, the posterior part of the metopic suture was still unossified (open) (Fig. 3D,E,G,H). In some *Icap-1*$^{-/-}$ mice, non-ossified, Alcian Blue-positive areas were observed extending from the posterior metopic suture to the frontal bones (Fig. 3E,H). Furthermore, the parietal bones were hypoplastic in

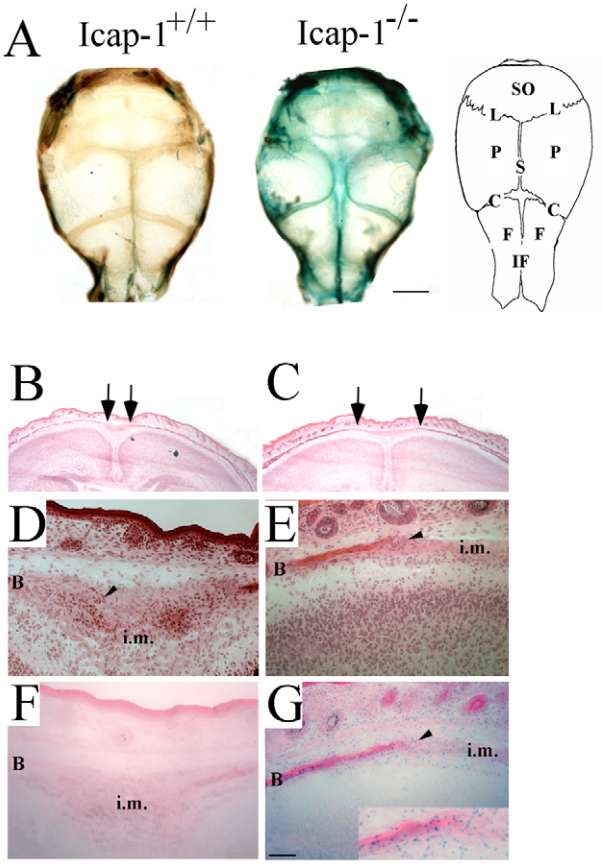

Fig. 4. Defective formation of the osteogenic front in *Icap-1*$^{-/-}$ calvaria. (**A**) Whole-mount *lacZ* staining of newborn calvariae of *Icap-1*$^{+/+}$ and *Icap-1*$^{-/-}$ mice. Strong β-gal activity visualizes *Icap-1* expression in the sutural regions and the edges of the bony plates of the *Icap-1*-deficient calvaria. (**B**,**C**) Hematoxylin and Eosin-stained frontal section of the parietal region. The distance between the ossified ends of the parietal bones (arrows) is wider in *Icap-1*$^{-/-}$ (C) compared with wild-type mice (B). (**D-G**) Frozen frontal sections through the sagittal suture of wild-type (D,F) and *Icap-1*$^{-/-}$ (E,G) animals stained with Hematoxylin and Eosin (D,E) or for β-gal activity (F,G). Note that the wild-type suture presents a typical condensed cell population corresponding to the osteogenic front (arrowheads) that is severely reduced in the *Icap-1*$^{-/-}$ mice. *lacZ* staining indicates extensive expression of ICAP-1 in this region. B, bone; i.m, intersutural mesenchyme; SO, supraoccipital bone; P, parietal bone; F, frontal bone; S, sagittal suture; L, lambdoid suture; C, coronal suture; IF, interfrontal suture. Scale bars: 2 mm in A; 50 μm in B-G.

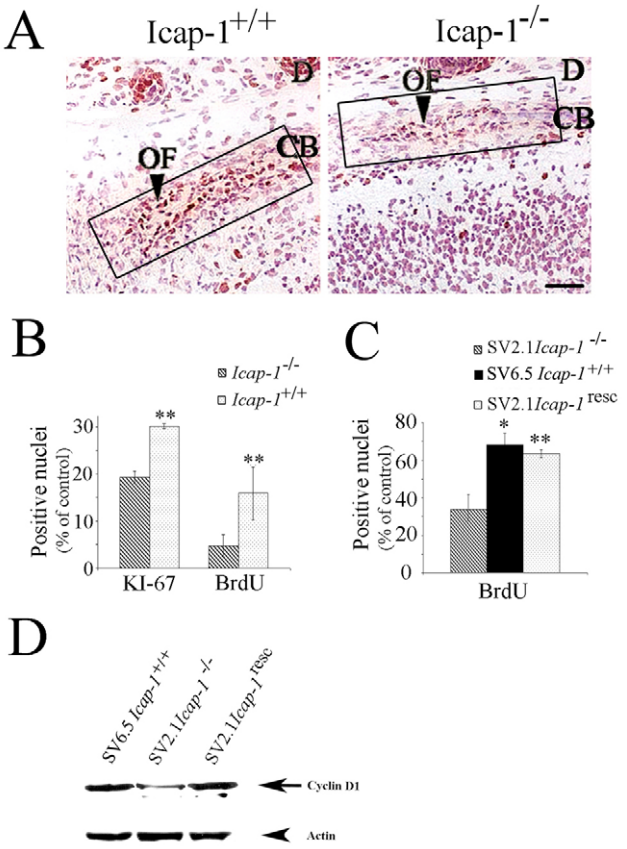

Fig. 5. Reduced proliferation of calvarial osteogenic cells in *Icap-1*-null mice. (**A**) Immunodetection of the proliferation marker Ki67 in the sagittal sutural region of newborn *Icap-1*$^{+/+}$ and *Icap-1*$^{-/-}$ calvaria. The osteogenic front of the *Icap-1*$^{-/-}$ mice displays a reduced number of Ki67-positive cells. Boxes indicate regions used for KI-67 and BrdU quantification in B. Scale bar: 25 μm. (**B**) Quantification of Ki67- and BrdU-positive cells in the osteogenic front of control and mutant animals. Error bars represent s.d.; asterisks indicate a statistically significant difference between *Icap-1*$^{+/+}$ and *Icap-1*$^{-/-}$ (**, P<0.0001). (**C**) Immortalized calvarial osteoblasts. ICAP-1-deficient cells (SV2.1-*Icap-1*$^{-/-}$) show significantly reduced BrdU-labeling index compared with wild-type cells (SV6.5-*Icap-1*$^{+/+}$). Retroviral transfection of the *Icap-1* cDNA into the *Icap-1*$^{-/-}$ cells rescues the proliferation defect (SV2.1-*Icap-1*^{resc}) (**, P<0.0001). (**D**) SV2.1 and SV2.1-*Icap-1*^{resc} cells were cultured for 24 hours in 1% FCS before replating them onto 10 μg/ml FN. After 5 hours of spreading, cells were washed with PBS and directly lysed onto Petri dishes with RIPA buffer. Protein (30 μg per lane) was gel separated and then transferred onto PVDF membrane before processing for western blotting with anti-cyclin D1 antibody. The same gel was blotted with anti-actin polyclonal antibodies for normalizing protein loading.

mutant calvarias leading to shortened sagittal and V-shaped coronal sutures. The bone defect was also evident in other parts of the skeleton, such as in the vertebrae, where 15-day-old mutant mice showed non-fused vertebral arches (Fig. 3I) and in the pelvic bone, where mutant mice showed delayed fusion of the pubis and the ischial bone (Fig. 3J).

Reduced proliferation of osteoprogenitors in calvarial bones

Since the skull vault is severely affected in *Icap-1*$^{-/-}$ mice, we decided to focus our analysis on the development of the calvaria. To test where ICAP-1 is expressed in the developing skull bones, we performed β-gal staining (Fig. 4A). Whole-mount staining of mutant calvariae revealed strong *lacZ* expression at the leading edges of the calvarial bones and in the suture regions (Fig. 4A). Frontal sections through the parietal region of the skull showed that the paired parietal bones from normal mice were separated at the midline by a narrow sagittal suture (Fig. 4B). However, in mutant mice the distance between the two parietal bones was wider without the typical suture organization (Fig. 4C). The sagittal suture is a fiber-rich stripe of mesenchyme flanked by condensed bulges of tissue called osteogenic fronts that contain the osteoprogenitors that differentiate into osteoblasts and lay down bone (Fig. 4D). In mutant mice, the osteogenic fronts were thin and contained very few cells

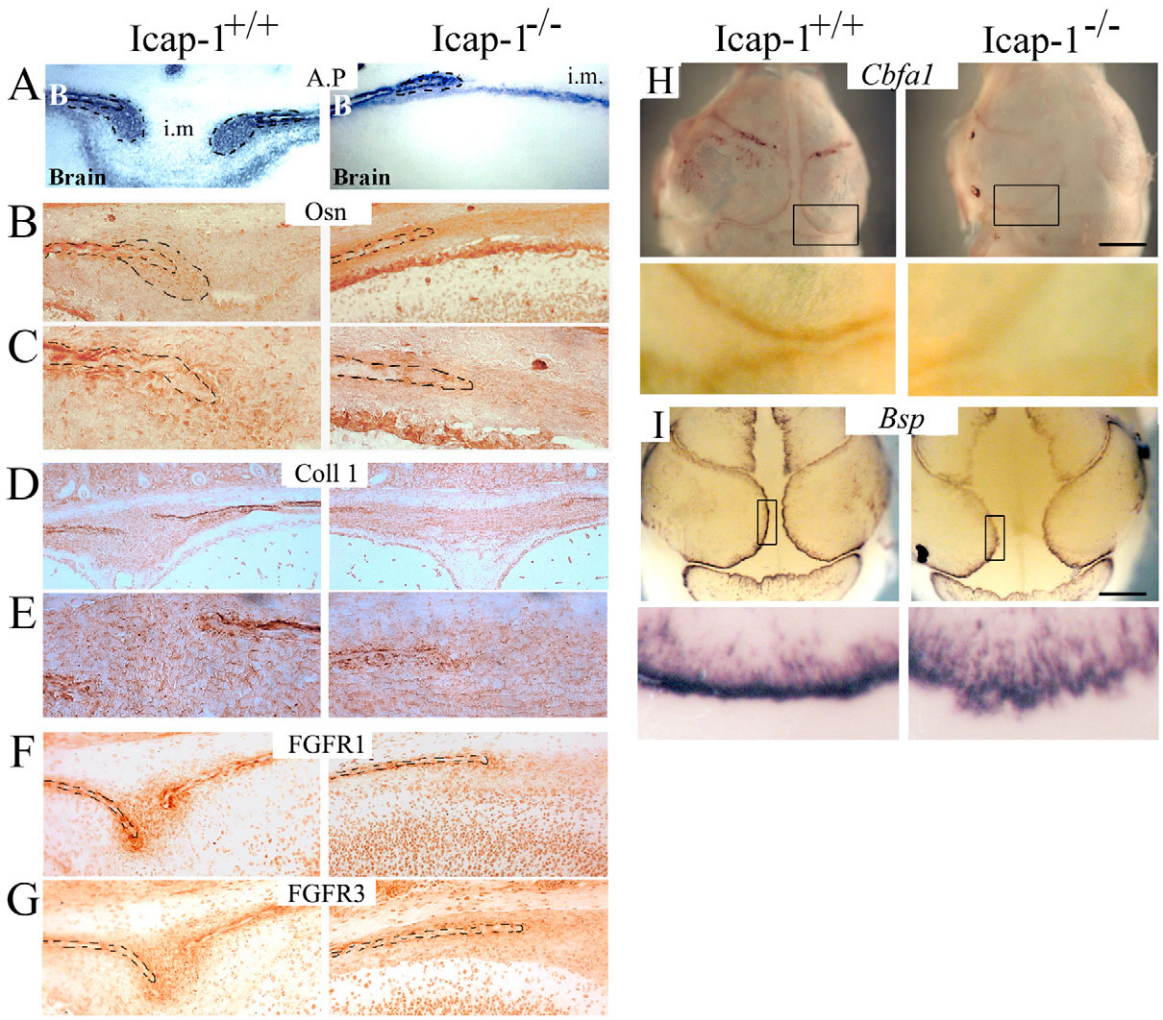

Fig. 6. Osteogenic differentiation is abnormal in *Icap-1*$^{-/-}$ calvaria. Frontal sections through the parietal bones and the sagittal suture of *Icap-1*$^{+/+}$ and *Icap-1*$^{-/-}$ newborn mice stained for (**A**) AP, (**B**,**C**) osteonectin, (**D**,**E**) COL1, (**F**) FGFR1 and (**G**) FGFR3. C and E are 400× magnification views of the osteogenic front region in B and D, respectively. Dashed lines represent bone borders and osteogenic front area. B, bone; i.m., intersutural mesenchyme. Note the reduced expression of the osteogenic and differentiation markers in *Icap-1*$^{-/-}$ tissue. (**H**,**I**) Whole-mount in situ hybridization on calvaria of E17.5 embryo was performed to detect either *Runx2* (*Cbfa1*) (H) or *Bsp* (I) transcripts in *Icap-1*$^{+/+}$ and *Icap-1*$^{-/-}$ embryos. The upper panel of each pair is an overview of the full calvaria; the lower panel is a closer view of the osteogenic front (boxed in the overview). Scale bars: 2 mm.

resulting in impaired growth of the parietal bones and widening of the intervening mesenchyme (Fig. 4C,E). β-gal staining revealed strong *Icap-1* promoter activity in mature osteoblasts of the parietal bone, in osteoprogenitors of the osteogenic fronts, and in mesenchymal cells between the two fronts (Fig. 4G). As expected, comparable tissue sections from wild-type mice showed no *lacZ* expression (Fig. 4F).

The morphogenesis of the calvaria depends on the number of osteoprogenitors and their differentiation into osteoblasts at the margins of the suture. To test whether the reduced number of osteoprogenitors in mutant osteogenic fronts was caused by aberrant cell survival and/or proliferation we performed apoptosis assays, BrdU incorporation assays and Ki67 immunostaining in newborn mice. The TUNEL assay and staining of activated caspase 3 showed very few apoptotic cells and similar in number for normal and mutant osteogenic fronts (data not shown). The labeling indexes for Ki67 and BrdU, however, were reduced in mutants by 40% and 64%, respectively, indicating a pronounced proliferation defect in the *Icap-1*-deficient osteoprogenitor cell population (Fig. 5A,B). Proliferation of osteoblast progenitor cells is tightly regulated by ECM interactions and growth factors. In order to determine whether the diminished proliferation at the osteogenic fronts are cell autonomous defects or caused by impaired secretion of growth factors and/or ECM components by the surrounding tissue, we isolated primary osteoblasts from the calvaria of control and mutant mice, immortalized them by retroviral transduction of the SV40 large T antigen, and tested their proliferation rates. Similar to the in vivo observations, *Icap-1*$^{-/-}$ cells (SV2.1-*Icap-1*$^{-/-}$) displayed a lower BrdU incorporation rate compared with control cells (SV6.5-*Icap-1*$^{+/+}$) in vitro (Fig. 5C). Retroviral infection of the full-length *Icap-1* cDNA into SV2.1-*Icap-1*$^{-/-}$ osteoblasts (SV2.1-*Icap-1*^{resc}) restored normal proliferation (Fig. 5C), corroborating the link between ICAP-1 loss and the proliferation defect. To further characterize the proliferation defect at the molecular level, we performed western blot analysis of cyclin D1 expression. Adhesion of wild-type or

rescued osteoblasts on FN led to increased cyclin D1 expression 5 hours after seeding. Conversely, *Icap-1*$^{-/-}$ preosteoblasts cultured under identical experimental conditions showed a significant reduction in cyclin D1 expression (Fig. 5D). These results indicate that the decreased (pre)osteoblast proliferation observed in *Icap-1*$^{-/-}$ mice is cell autonomous.

Calvarial osteogenesis is perturbed in *Icap-1*-deficient mice

The differentiation of osteoprogenitors into mature osteoblasts is characterized by the deposition of 'bone-specific' ECM molecules, as well as the spatially and temporally coordinated expression of growth and transcription factors. To study the cranial skeletogenic differentiation in *Icap-1*$^{-/-}$ mice, we first evaluated the expression of osteogenic markers such as alkaline phosphatase (AP), osteonectin (SPARC – Mouse Genome Informatics) and collagen type I (COL1) on frontal sections of newborn calvariae (Fig. 6). In the wild type, AP activity was confined to the osteoid region of the developing parietal bones and to preosteoblasts at the osteogenic front of the sagittal suture (Fig. 6A). Osteonectin expression overlapped with sites of AP activity (Fig. 6B,C) and was strong along the bone surface and weak in cells at the osteogenic front. In mutant tissue, the cell number with AP activity was reduced at the bone-suture margins, defining a smaller osteogenic front area committed to osteoblastic differentiation (Fig. 6A). Osteonectin deposition was also reduced at the osteoid surface and was almost absent at the osteogenic front (Fig. 6B,C). Similarly, COL1 immunostaining was markedly reduced on the bone surface and at the suture margin in the mutant compared with the wild type (Fig. 6D,E).

Since the expression patterns of FGF-receptors correlate with the osteogenic differentiation process (Iseki et al., 1999; Rice et al., 2000), we compared the expression of FGFR1 and FGFR3 in wild-type and mutant newborn calvariae. In control tissue, both proteins were detected in the osteoblasts of the calvarial bones and in cells of the osteogenic front and weakly in the sutural mesenchyme (Fig. 6F,G). In *Icap-1*$^{-/-}$ calvariae, FGFR1 and FGFR3 immunolabeling was fainter than in wild type, and this difference was particularly pronounced at the osteogenic fronts (Fig. 6F,G). In addition, whole-mount in situ hybridization on E17.5 heads revealed that the expression of both the early bone marker *Runx2* (*Cbfa1*) and the later marker bone sialic protein (*Bsp*; *Ibsp* – Mouse Genome Informatics) were reduced in mutant mice (Fig. 6H,I). Again, a weaker signal was observed at the edge of the bony region, reflecting the marked reduction of cells committed into the osteoblastic lineage within the osteogenic front. Altogether, these results indicate that the osteogenic front is not normally formed in mutant animals.

To test whether committed cells differentiate normally, primary osteoblasts were isolated from newborn wild-type and *Icap-1*$^{-/-}$ calvariae and incubated in medium supplemented with ascorbic acid and β-glycerophosphate to induce osteoblast differentiation and the formation of mineralized bone nodules (Fig. 7A). After 2 weeks in the differentiation medium, AP activity was evident in almost all cells derived from control calvariae indicating their commitment to the osteoblast lineage. *Icap-1*$^{-/-}$ calvarial cells also started to express AP, albeit at lower levels (data not shown). After 4 weeks of culture, differentiating osteoblasts from *Icap-1*$^{-/-}$ calvariae contained fewer and smaller mineralized nodules as visualized by Alizarin Red (Fig. 7A) and von Kossa staining (data not shown). Similarly, immortalized *Icap-1*$^{-/-}$ cells (SV2.1-*Icap-1*$^{-/-}$) showed markedly reduced AP staining and mineralized

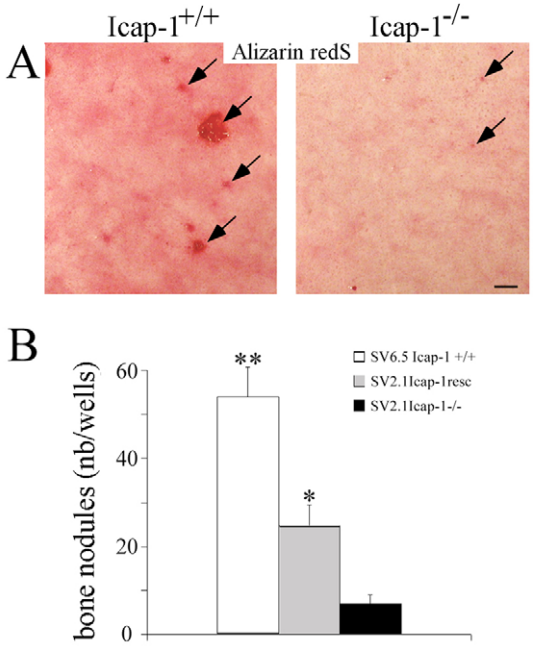

Fig. 7. Bone nodule formation by the calvarial osteoblast is defective in *Icap-1*$^{-/-}$ mice. (**A**) Primary *Icap-1*$^{+/+}$ and *Icap-1*-deficient osteoblasts were cultured for 4 weeks in inductive medium and stained with Alizarin Red for monitoring bone nodule formation. *Icap-1*$^{-/-}$ cultures show fewer and smaller mineralized nodules (arrows) compared with wild-type cultures (*Icap-1*$^{+/+}$). The result is representative of at least three independent experiments from three different animals. Scale bar: 1 mm. (**B**) Immortalized osteoblasts SV2.1 *Icap-1*$^{-/-}$, SV6.5 *Icap-1*$^{+/+}$ or SV2.1-*Icap-1*^{resc} were cultured in inductive medium for 3 weeks and mineralized nodules were identified by Alizarin Red staining. *Icap-1*$^{-/-}$ osteoblasts show a significantly reduced nodule formation compared with wild-type or *Icap-1*^{resc} osteoblasts. The means and s.d. were calculated from three independent experiments (*, $P<0.05$; **, $P<0.0001$).

nodule formation relative to wild-type (SV6.5-*Icap-1*$^{+/+}$) and rescued cells (SV2.1-*Icap-1*^{resc}) (Fig. 7B and data not shown). These data show that ICAP-1 loss impairs osteogenesis and identifies a role of ICAP-1 as a cell-autonomous factor in osteoblast differentiation.

Since we routinely induced differentiation after cells derived from calvariae or immortalized osteoprogenitors had reached confluence in vitro, the numbers of neither the mutant (SV2.1-*Icap-1*$^{-/-}$) nor the wild-type (SV6.5-*Icap-1*$^{+/+}$) or rescued cells (SV2.1-*Icap-1*^{resc}) significantly increased during the differentiation period (data not shown). Altogether, these findings suggest that the differentiation block occurs in addition to the cell proliferation defect.

β_1 integrin is highly expressed and activated in osteogenic front

β_1 integrins have been proposed to play a crucial role during osteoblast proliferation and differentiation (Moursi et al., 1997; Zimmerman et al., 2000). Since ICAP-1 interacts with the cytoplasmic tail of the β_1 integrin chain and modulates integrin function in vitro (Bouvard et al., 2003), we analyzed β_1 integrin expression in wild-type and mutant calvariae in vivo. At newborn stage, frontal sections through the sagittal suture and the parietal bones were immunostained with an anti-β_1 polyclonal antibody and with the monoclonal antibody 9EG7, which recognizes the ligand-bound form of β_1 integrins (Fig. 8A and data not shown). In sections

from control mice, both antibodies strongly labeled the osteogenic fronts and the bone surfaces, whereas the intervening mesenchyme was faintly labeled. Conversely, sections from *Icap-1*-deficient mice showed clear β_1 integrin staining of the bone surface but very faint staining of cells at the osteogenic front. This apparently diminished β_1 staining was mainly due to the reduced osteogenic front population, rather than reduced expression on the cell surface of individual cells, because FACS analysis showed only a slight reduction of β_1 integrin expression on *Icap-1*$^{-/-}$ osteoblasts (Fig. 8B, see below).

ICAP-1 controls β_1 integrin activity and condensation of osteoprogenitors

To further analyze the consequence of ICAP-1 expression loss for the adhesion of osteoblasts, assays were carried out using primary osteoblasts isolated from calvarial tissues. Despite a small decrease in β_1 expression (Fig. 8B), adhesion of *Icap-1*$^{-/-}$ osteoblasts to FN or COL1 was moderately but significantly increased compared with wild-type osteoblasts (Fig. 8C). This suggests that increased adhesion to ECM substrates resulted from the activation, rather than an increased cell surface expression, of β_1 integrins on *Icap-1*$^{-/-}$ osteoblasts.

To investigate whether the loss of ICAP-1 expression interferes with integrin activation, we estimated the ligand-binding affinity of the FN receptor $\alpha_5\beta_1$ integrin both in wild-type and *Icap-1*$^{-/-}$ primary osteoblasts. The cell-binding domain of FN, corresponding to the type III repeats 7-10 (Fn7-10), was expressed, purified and FITC-labeled. The capability of both mutant and wild-type primary osteoblast cells to interact with Fn7-10 at a non-saturating concentration was analyzed by FACS. As shown in Fig. 8D, we consistently observed an increase in Fn7-10 binding to *Icap-1*$^{-/-}$ osteoblasts compared with wild-type cells. The activation index, which normalizes the specific binding of FITC–Fn7-10 to the total β_1 surface expression level, was elevated by approximately three-fold in *Icap-1*$^{-/-}$ as compared with wild-type cells (Fig. 8E).

During in vitro differentiation of both primary and immortalized osteoblasts, we consistently observed that the bone nodules formed by *Icap-1*$^{-/-}$ cells were fewer, smaller and less compact than those formed by wild-type cells (Fig. 9A). As differentiation of bone cells requires an initial step of cell condensation (Globus et al., 1998; Ornitz and Marie, 2002), a defect in this step might lead to altered or delayed differentiation. To address this question, we cultured immortalized osteoprogenitors in suspension using the hanging drop technique. Under these conditions, wild-type or rescued cells aggregated and formed compact spheroids within 48 hours, whereas spheroids formed by *Icap-1*$^{-/-}$ cells were less compacted (Fig. 9B and data not shown).

Since ICAP-1 loss increases integrin affinity (Fig. 8), we investigated whether blocking of β_1 integrins in their activated state would mimic ICAP-1 deficiency. To this end, we complemented the culture medium with the integrin-activating monoclonal antibody 9EG7 and then formed spheroids (Fig. 9B). Whereas spheroid-triggered compaction of *Icap-1*$^{-/-}$ cells was not affected by treatment with the 9EG7 antibody, compaction of control or rescued cells was consistently delayed. These findings indicate that modulation of integrin affinity by ICAP-1 is required for proper compaction of osteoblastic cells.

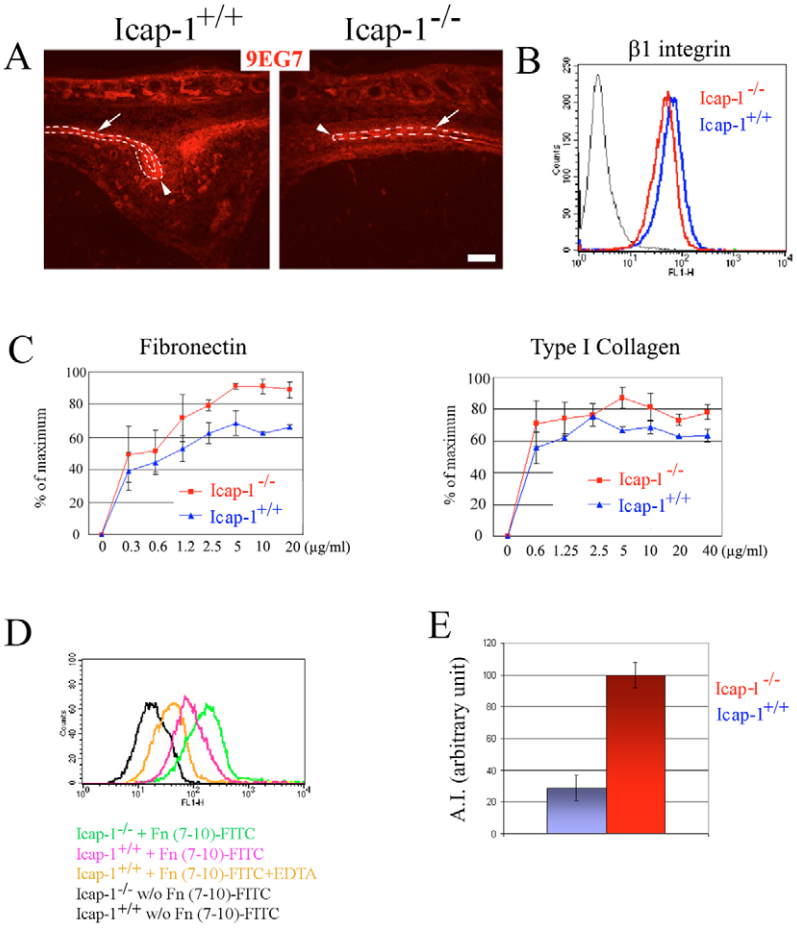

Fig. 8. Increases in β_1 integrin activity in *Icap-1*$^{-/-}$ mouse cells. (**A**) Sagittal sections were stained with the 9EG7 monoclonal antibody (red) that recognizes ligand-bound β_1 integrins. β_1 integrins are highly expressed and strongly activated in wild-type cells (*Icap-1*$^{+/+}$) at the osteogenic front (arrowheads) and at the surface of the bony plates (arrows). In *Icap-1*$^{-/-}$ tissues, the cells at the osteogenic front show a moderate staining for activated β_1 integrin. Scale bar: 50 μm. (**B**) FACS analyses demonstrate a slight reduction in the surface expression of β1 integrins (assayed by the MB1.2 monoclonal antibody) on *Icap-1*$^{-/-}$ primary osteoblasts (red) compared with wild-type osteoblasts (blue). (**C**) Adhesion assays. The adhesion of *Icap-1*$^{-/-}$ primary osteoblasts to FN and COL1 is moderately increased compared with that of *Icap-1*$^{+/+}$ cells. Adhesion is expressed as a percentage of the maximal adhesion and measured in duplicate in two independent experiments from two different animals (P<0.05). (**D**) FACS analysis demonstrates increased binding of FITC-Fn7-10 fragment to *Icap-1*$^{-/-}$ osteoblasts (green). (**E**) The activation index (AI) of the β_1 integrin is increased in *Icap-1*$^{-/-}$ osteoblats. The maximum AI obtained is used to normalize both genotype groups and designated as 100.

DISCUSSION

We report the molecular analysis of mice carrying a disrupted *Icap-1* gene. *Icap-1*-deficient mice suffer from defective osteogenesis characterized by mild growth retardation and severe craniofacial dysmorphism. We focused our analyses on the calvarial abnormalities to obtain a clear view of osteoblast differentiation.

ICAP-1 plays an important role for osteogenesis

Bone formation (osteogenesis) involves the conversion of mesenchymal tissue into bone, either directly (intramembranous ossification) or via cartilaginous intermediates (endochondral ossification) (Zelzer and Olsen, 2003). The first mechanism is responsible for the generation of the flat bones of the skull vault as well as for the formation of the bony collar around the diaphysis of the long bones. In *Icap-1*$^{-/-}$ mice, intramembranous ossification is affected, as both periosteal and calvarial osteogenesis are delayed. Alcian Blue staining revealed that the formation of cartilaginous templates of endochondral bones is grossly undisturbed in mutant mice. Since ICAP-1 is also expressed in chondrocytes (data not shown), we cannot fully exclude mild differentiation and/or proliferation defects of mutant chondrocytes, which might also contribute to the small stature of *Icap-1*$^{-/-}$ mice. We focused our investigations on intramembranous ossification and show for the first time the important role of ICAP-1 during osteoblast differentiation. The ossification of calvarial bones (frontal, parietal and interfrontal) was dramatically delayed during embryonic development, leading to open fontanels and wide sutures at birth. These symptoms mirror the calvarial abnormalities of mice carrying mutations for the transcription factors *Runx2* (Otto et al., 1997) and *Atf4* (Yang et al., 2004), which have been identified as key regulators of osteoblast differentiation. The remarkable phenotypic similarities between the *Icap-1*$^{-/-}$ mice and these mouse models suggest that ICAP-1 is a newly recognized and important regulator of osteoblast development. Cranial sutures regulate bone expansion during postnatal life and remain non-ossified as long as the brain is growing (Opperman, 2000). Osteogenesis at the suture involves the differentiation of mesenchymal cells into preosteoblasts and into osteoblasts at the sutural margins and the subsequent deposition of a collagenous matrix along the bony plates. Increased growth of the calvarial bones leads to premature closure of the sutures (craniosynostoses), whereas delayed bone growth results in suture latency. ICAP-1 is expressed at the osteogenic fronts and its deficiency leads to a dramatic reduction in the osteoblast population at the osteogenic fronts, which in turn prevents correct temporal fusion of cranial sutures. The reduced osteoblast number at the osteogenic fronts is due to reduced proliferation and impaired osteoblast differentiation.

ICAP-1 regulates osteoblast proliferation

We have previously reported that ICAP-1 has a dual localization and is found in the cytoplasm/membrane and in the nucleus (Fournier et al., 2005). Loss of ICAP-1 expression in immortalized osteoblasts considerably reduced cell proliferation and cyclin D1 expression. Therefore, the reduced proliferation in the osteogenic front is likely to result from a lack of ICAP-1 in the nucleus, which would lead to reduced cyclin D1 expression. This might explain the severe decrease in the cell population committed to the osteoblast lineage in the sutural region that we observed in the *Icap-1*-deficient animals.

ICAP-1 regulates integrin activity

Isolated *Icap-1*-null primary osteoblasts displayed an increased cell adhesion to FN and COL1. We have previously shown that overexpression of ICAP-1 in HeLa cells disrupts focal adhesion, probably by inhibiting the association of the cytoplasmic tail of β_1 integrin with talin (Bouvard et al., 2003). It has been shown that talin binding to the β integrin domain is a key step in the regulation of integrin activation (Calderwood et al., 2004; Calderwood et al., 2002). In good agreement with this, we found an increase in Fn7-10 binding to integrin in mutant cells that was not accompanied by any upregulation of β_1 integrin expression. This confirms that ICAP-1 regulates β_1 integrin affinity.

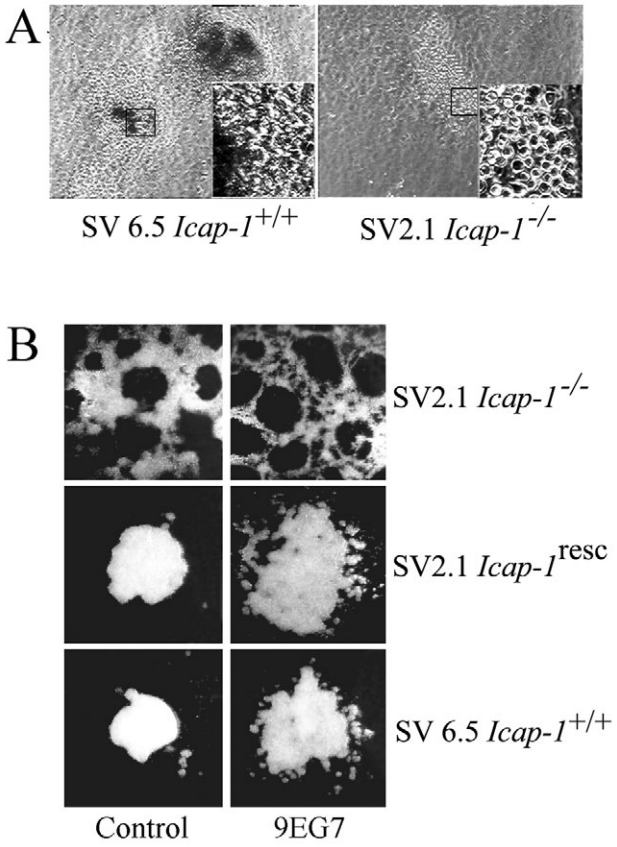

Fig. 9. Defects in bone nodule formation and spheroid compaction with *Icap-1*$^{-/-}$ osteoblasts. (**A**) Immortalized SV6.5 (wild-type) or SV2.1 (*Icap-1*$^{-/-}$) preosteoblasts were induced to differentiate in vitro for 15 days, then bone nodule formation and organization were visualized by phase contrast microscopy. The inset is a higher magnification view of the boxed region. Note that SV2.1 cells are less cohesive than control cells. (**B**) Spheroids were formed from SV2.1, from SV2.1 rescued with *Icap-1* cDNA or from SV6.5 preosteoblasts and analyzed after 16 hours incubation at 37°C using a standard protocol for the hanging drop assay. We used 25,000 cells per drop in each experimental condition. For antibody treatment, 9EG7 or control antibodies were added at a final concentration of 10 μg/ml during the condensation process in a medium supplemented with an FN-depleted serum. Note that cellular compaction is delayed in both *Icap-1*$^{-/-}$ and 9EG7-treated wild-type osteoblast compared with untreated wild-type cells.

ICAP-1 regulates osteoblast differentiation

Osteoblast differentiation is a multistep process that first required an initial condensation of the mesenchymal cells to form the osteogenic front (Fig. 10) (Hall and Miyake, 2000). The cell population at the osteogenic front is visible during calvaria bone development at the edge of the expanding bone within the intervening mesenchyme. This condensed cell population further differentiates and expresses

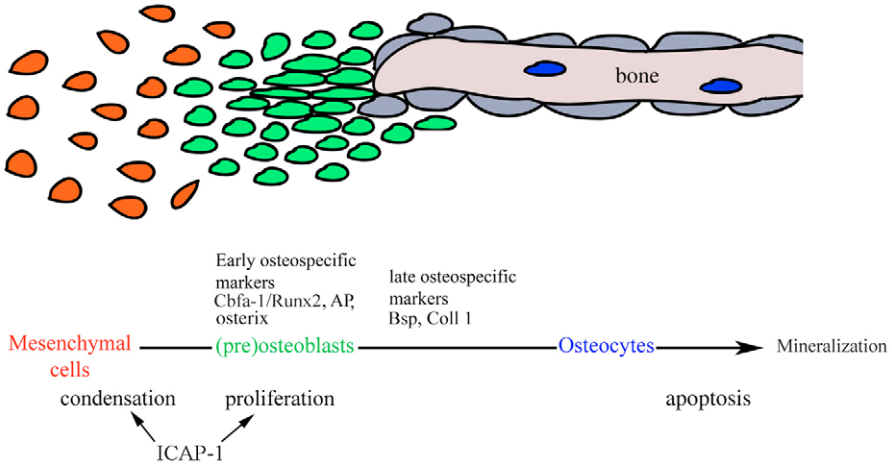

Fig. 10. Schematic representation of bone formation in calvaria. Bone formation is a multistep process that requires an initial condensation stage. In this step, which enables the cells to start the differentiation process, early markers such as RUNX2 and osterix (also known as SP7) are expressed. At later stages, other osteogenic markers such as BSP, osteocalcin (also known as BGLAP) and osteonectin are produced. Lack of ICAP-1 expression slows down proliferation and the ability of mesenchymal cells to compact. Since the compaction is a very early event in the osteoblast differentiation pathway, the expression of more-distal markers is consequently reduced in *Icap-1*$^{-/-}$ mice.

different osteoblastic markers including RUNX2, AP and BSP. Our knowledge of how integrins or cell adhesion is implicated into this process is poorly documented, but recent reports suggested an unexpected role for matrix stiffness in controlling early osteoblast differentiation (Engler et al., 2006; McBeath et al., 2004).

It has also been reported that β_1 integrins play an important role in osteoblast differentiation in vitro. It was shown that COL1 interaction with $\alpha_2\beta_1$ integrin regulates osteoblast-specific gene expression and osteoblast differentiation (Takeuchi et al., 1996; Xiao et al., 1998). Similarly, $\alpha_5\beta_1$ integrin interaction with FN promotes differentiation (Moursi et al., 1997) and survival (Globus et al., 1998) of cultured calvarial osteoblasts. Finally, transgenic overexpression of a dominant-negative form of β_1 integrin in osteocytes blocks β_1 integrin function, reduces adhesion to collagen and FN, and diminishes bone mass in cortical and flat bones (Zimmerman et al., 2000). Although these studies identify an important role for β_1 integrins for osteogenesis, they do not address the role of integrin affinity modulation in bone development. Our data demonstrate for the first time that not only β_1 integrin affinity increases, but also affinity decreases, are of paramount importance for proper bone development both in vivo and in vitro.

We consistently observed a marked reduction of osteoblast cells in *Icap-1*-deficient animals. Even the expression of the very early marker RUNX2 at the osteogenic front region was significantly reduced. Furthermore, the in vitro differentiation assays revealed that the bone nodules formed by *Icap-1*-null immortalized osteoprogenitors were smaller and less compacted as compared with nodules formed from wild-type or rescued cells. This reduced compaction of *Icap-1*-deficient cells was further confirmed by the hanging drop technique, suggesting that ICAP-1 is required for osteoblast condensation, which is a crucial and early step during osteoblast differentiation.

Our data suggest that the proliferation and the differentiation defects occur independently and that they both contribute to the abnormal osteogenesis. In support for this notion, we observed that limited ICAP-1 expression in *Icap-1*-deficient preosteoblast cell lines fully restored their proliferation rate, but only partially their potential to differentiate and form nodules in vitro. Furthermore, in our differentiation assay, we routinely use confluent cells to rule out the possibility that the proliferation defect is influencing the formation of mineralized nodules. Indeed, we observed only a slight increase in cells during the differentiation period and this increase was similar in control and *Icap-1*-deficient cultures. Our data indicate that the condensation defect of the *Icap-1*-deficient preosteoblasts further limits the number of progenitors that will finally differentiate into mature osteoblasts (Fig. 9). The functional importance of the condensation of progenitors for osteoblast development has also been observed in connexin 43 (GJA1)-deficient mice (Lecanda et al., 2000).

Previous work implicated β_1 integrins in cell compaction (Robinson et al., 2004; Robinson et al., 2003). Our data suggest that ICAP-1 might control β_1 integrin function during this process by regulating activation/deactivation cycles. To our knowledge this is the first direct evidence reporting that integrin affinity is important for cell cohesion and differentiation.

We thank Drs R. Timpl, S. Johannsonn, B. Nieswandt, C. Bosco and G. Karsenty for generously providing antibodies and in situ probes; C. Robert-Coutant and J. M. Dinten for X-ray imaging of mice; V. Collin for cell sorting and P. Marie, M. Pfaff and D. Pearton for valuable discussions and critical reading of the manuscript. D.B. was supported by an E.C. Marie Curie long-term fellowship (QLGA-CT-2000-52076), the Association pour la Recherche contre le Cancer (ARC), the CNRS and the Max Planck Society. R.F. is supported by the DFG, BMBF and the Max Planck Society. This work is dedicated to the memory of Rupert Timpl, Günter Kostka, Martin Pfaff and Christine Robert-Coutant.

References

Aszodi, A., Chan, D., Hunziker, E., Bateman, J. F. and Fassler, R. (1998). Collagen II is essential for the removal of the notochord and the formation of intervertebral discs. *J. Cell Biol.* **143**, 1399-1412.

Bellows, C. G., Aubin, J. E., Heersche, J. N. and Antosz, M. E. (1986). Mineralized bone nodules formed in vitro from enzymatically released rat calvaria cell populations. *Calcif. Tissue Int.* **38**, 143-154.

Bos, J. L., de Rooij, J. and Reedquist, K. A. (2001). Rap1 signalling: adhering to new models. *Nat. Rev. Mol. Cell Biol.* **2**, 369-377.

Bouvard, D. and Block, M. R. (1998). Calcium/calmodulin-dependent protein kinase II controls integrin alpha5beta1-mediated cell adhesion through the integrin cytoplasmic domain associated protein-1alpha. *Biochem. Biophys. Res. Commun.* **252**, 46-50.

Bouvard, D., Molla, A. and Block, M. R. (1998). Calcium/calmodulin-dependent protein kinase II controls alpha5beta1 integrin-mediated inside-out signaling. *J. Cell Sci.* **111**, 657-665.

Bouvard, D., Vignoud, L., Dupe-Manet, S., Abed, N., Fournier, H. N., Vincent-Monegat, C., Retta, S. F., Fassler, R. and Block, M. R. (2003). Disruption of focal adhesions by integrin cytoplasmic domain-associated protein-1 alpha. *J. Biol. Chem.* **278**, 6567-6574.

Brakebusch, C., Bouvard, D., Stanchi, F., Sakai, T. and Fassler, R. (2002). Integrins in invasive growth. *J. Clin. Invest.* **109**, 999-1006.

Calderwood, D. A. (2004). Integrin activation. *J. Cell Sci.* **117**, 657-666.

Calderwood, D. A., Yan, B., de Pereda, J. M., Alvarez, B. G., Fujioka, Y., Liddington, R. C. and Ginsberg, M. H. (2002). The phosphotyrosine binding-like domain of talin activates integrins. *J. Biol. Chem.* **277**, 21749-21758.

Calderwood, D. A., Tai, V., Di Paolo, G., De Camilli, P. and Ginsberg, M. H. (2004). Competition for talin results in trans-dominant inhibition of integrin activation. *J. Biol. Chem.* **279**, 28889-28895.

Chang, D. D., Wong, C., Smith, H. and Liu, J. (1997). ICAP-1, a novel beta1

integrin cytoplasmic domain-associated protein, binds to a conserved and functionally important NPXY sequence motif of beta1 integrin. *J. Cell Biol.* **138**, 1149-1157.

Degani, S., Balzac, F., Brancaccio, M., Guazzone, S., Retta, S. F., Silengo, L., Eva, A. and Tarone, G. (2002). The integrin cytoplasmic domain-associated protein ICAP-1 binds and regulates Rho family GTPases during cell spreading. *J. Cell Biol.* **156**, 377-387.

Engler, A. J., Sen, S., Sweeney, H. L. and Discher, D. E. (2006). Matrix elasticity directs stem cell lineage specification. *Cell* **126**, 677-689.

Faisst, A. M. and Gruss, P. (1998). Bodenin: a novel murine gene expressed in restricted areas of the brain. *Dev. Dyn.* **212**, 293-303.

Fässler, R., Pfaff, M., Murphy, J., Noegel, A. A., Johansson, S., Timpl, R. and Albrecht, R. (1995). Lack of beta 1 integrin gene in embryonic stem cells affects morphology, adhesion, and migration but not integration into the inner cell mass of blastocysts. *J. Cell Biol.* **128**, 979-988.

Fournier, H. N., Dupe-Manet, S., Bouvard, D., Lacombe, M. L., Marie, C., Block, M. R. and Albiges-Rizo, C. (2002). Integrin cytoplasmic domain-associated protein 1alpha (ICAP-1alpha) interacts directly with the metastasis suppressor nm23-H2, and both proteins are targeted to newly formed cell adhesion sites upon integrin engagement. *J. Biol. Chem.* **277**, 20895-20902.

Fournier, H. N., Dupe-Manet, S., Bouvard, D., Luton, F., Degani, S., Block, M. R., Retta, S. F. and Albiges-Rizo, C. (2005). Nuclear translocation of integrin cytoplasmic domain-associated protein 1 stimulates cellular proliferation. *Mol. Biol. Cell* **16**, 1859-1871.

Globus, R. K., Doty, S. B., Lull, J. C., Holmuhamedov, E., Humphries, M. J. and Damsky, C. H. (1998). Fibronectin is a survival factor for differentiated osteoblasts. *J. Cell Sci.* **111**, 1385-1393.

Gunel, M., Laurans, M. S., Shin, D., DiLuna, M. L., Voorhees, J., Choate, K., Nelson-Williams, C. and Lifton, R. P. (2002). KRIT1, a gene mutated in cerebral cavernous malformation, encodes a microtubule-associated protein. *Proc. Natl. Acad. Sci. USA* **99**, 10677-10682.

Hall, B. K. and Miyake, T. (2000). All for one and one for all: condensations and the initiation of skeletal development. *BioEssays* **22**, 138-147.

Hynes, R. O. (1992). Integrins: versatility, modulation, and signaling in cell adhesion. *Cell* **69**, 11-25.

Hynes, R. O. (2002). Integrins: bidirectional, allosteric signaling machines. *Cell* **110**, 673-687.

Iseki, S., Wilkie, A. O. and Morriss-Kay, G. M. (1999). Fgfr1 and Fgfr2 have distinct differentiation- and proliferation-related roles in the developing mouse skull vault. *Development* **126**, 5611-5620.

Laberge-le Couteulx, S., Jung, H. H., Labauge, P., Houtteville, J. P., Lescoat, C., Cecillon, M., Marechal, E., Joutel, A., Bach, J. F. and Tournier-Lasserve, E. (1999). Truncating mutations in CCM1, encoding KRIT1, cause hereditary cavernous angiomas. *Nat. Genet.* **23**, 189-193.

Lecanda, F., Warlow, P. M., Sheikh, S., Furlan, F., Steinberg, T. H. and Civitelli, R. (2000). Connexin43 deficiency causes delayed ossification, craniofacial abnormalities, and osteoblast dysfunction. *J. Cell Biol.* **151**, 931-944.

Mansukhani, A., Bellosta, P., Sahni, M. and Basilico, C. (2000). Signaling by fibroblast growth factors (FGF) and fibroblast growth factor receptor 2 (FGFR2)-activating mutations blocks mineralization and induces apoptosis in osteoblasts. *J. Cell Biol.* **149**, 1297-1308.

McBeath, R., Pirone, D. M., Nelson, C. M., Bhadriraju, K. and Chen, C. S. (2004). Cell shape, cytoskeletal tension, and RhoA regulate stem cell lineage commitment. *Dev. Cell* **6**, 483-495.

Moursi, A. M., Globus, R. K. and Damsky, C. H. (1997). Interactions between integrin receptors and fibronectin are required for calvarial osteoblast differentiation in vitro. *J. Cell Sci.* **110**, 2187-2196.

Opperman, L. A. (2000). Cranial sutures as intramembranous bone growth sites. *Dev. Dyn.* **219**, 472-485.

Ornitz, D. M. and Marie, P. J. (2002). FGF signaling pathways in endochondral and intramembranous bone development and human genetic disease. *Genes Dev.* **16**, 1446-1465.

Otto, F., Thornell, A. P., Crompton, T., Denzel, A., Gilmour, K. C., Rosewell, I. R., Stamp, G. W., Beddington, R. S., Mundlos, S., Olsen, B. R. et al. (1997). Cbfa1, a candidate gene for cleidocranial dysplasia syndrome, is essential for osteoblast differentiation and bone development. *Cell* **89**, 765-771.

Otto, T. E., Nulend, J. K., Patka, P., Burger, E. H. and Haarman, H. J. (1996). Effect of (poly)-L-lactic acid on the proliferation and differentiation of primary bone cells in vitro. *J. Biomed. Mater. Res.* **32**, 513-518.

Rice, D. P., Aberg, T., Chan, Y., Tang, Z., Kettunen, P. J., Pakarinen, L., Maxson, R. E. and Thesleff, I. (2000). Integration of FGF and TWIST in calvarial bone and suture development. *Development* **127**, 1845-1855.

Robinson, E. E., Zazzali, K. M., Corbett, S. A. and Foty, R. A. (2003). Alpha5beta1 integrin mediates strong tissue cohesion. *J. Cell Sci.* **116**, 377-386.

Robinson, E. E., Foty, R. A. and Corbett, S. A. (2004). Fibronectin matrix assembly regulates alpha5beta1-mediated cell cohesion. *Mol. Biol. Cell* **15**, 973-981.

Sakai, K., Hiripi, L., Glumoff, V., Brandau, O., Eerola, R., Vuorio, E., Bosze, Z., Fassler, R. and Aszodi, A. (2001). Stage-and tissue-specific expression of a Col2a1-Cre fusion gene in transgenic mice. *Matrix Biol.* **19**, 761-767.

Serebriiskii, I., Estojak, J., Sonoda, G., Testa, J. R. and Golemis, E. A. (1997). Association of Krev-1/rap1a with Krit1, a novel ankyrin repeat-containing protein encoded by a gene mapping to 7q21-22. *Oncogene* **15**, 1043-1049.

Takeuchi, Y., Nakayama, K. and Matsumoto, T. (1996). Differentiation and cell surface expression of transforming growth factor-beta receptors are regulated by interaction with matrix collagen in murine osteoblastic cells. *J. Biol. Chem.* **271**, 3938-3944.

Talts, J. F., Brakebusch, C. and Fassler, R. (1999). Integrin gene targeting. *Methods Mol. Biol.* **129**, 153-187.

Vinogradova, O., Velyvis, A., Velyviene, A., Hu, B., Haas, T., Plow, E. and Qin, J. (2002). A structural mechanism of integrin alpha(IIb)beta(3) "inside-out" activation as regulated by its cytoplasmic face. *Cell* **110**, 587-597.

Xiao, G., Wang, D., Benson, M. D., Karsenty, G. and Franceschi, R. T. (1998). Role of the alpha2-integrin in osteoblast-specific gene expression and activation of the Osf2 transcription factor. *J. Biol. Chem.* **273**, 32988-32994.

Yang, X., Matsuda, K., Bialek, P., Jacquot, S., Masuoka, H. C., Schinke, T., Li, L., Brancorsini, S., Sassone-Corsi, P., Townes, T. M. et al. (2004). ATF4 is a substrate of RSK2 and an essential regulator of osteoblast biology; implication for Coffin-Lowry Syndrome. *Cell* **117**, 387-398.

Zawistowski, J. S., Serebriiskii, I. G., Lee, M. F., Golemis, E. A. and Marchuk, D. A. (2002). KRIT1 association with the integrin-binding protein ICAP-1: a new direction in the elucidation of cerebral cavernous malformations (CCM1) pathogenesis. *Hum. Mol. Genet.* **11**, 389-396.

Zelzer, E. and Olsen, B. R. (2003). The genetic basis for skeletal diseases. *Nature* **423**, 343-348.

Zhang, J., Clatterbuck, R. E., Rigamonti, D., Chang, D. D. and Dietz, H. C. (2001). Interaction between krit1 and icap1alpha infers perturbation of integrin beta1-mediated angiogenesis in the pathogenesis of cerebral cavernous malformation. *Hum. Mol. Genet.* **10**, 2953-2960.

Zhang, X. A. and Hemler, M. E. (1999). Interaction of the integrin beta1 cytoplasmic domain with ICAP-1 protein. *J. Biol. Chem.* **274**, 11-19.

Zimmerman, D., Jin, F., Leboy, P., Hardy, S. and Damsky, C. (2000). Impaired bone formation in transgenic mice resulting from altered integrin function in osteoblasts. *Dev. Biol.* **220**, 2-15.